arXiv:1411.3518v1 [hep-ph] 13 Nov 2014

Elastic Amplitudes and Observables in pp Scattering

A. Kendi Kohara, Erasmo Ferreira and Takeshi Kodama

Instituto de Física, Universidade Federal do Rio de Janeiro, C.P. 68528, Rio de Janeiro 21945-970, RJ, Brazil

Abstract.
Using a unified analytic representation for the elastic scattering amplitudes of pp scattering valid for all high energy region, the behavior of observables in the LHC collisions in the range $\sqrt{s}$ = 2.76 - 14 TeV is discussed. Similarly to the case of 7 TeV data, the proposed amplitudes give excellent description of the preliminary 8 TeV data. We discuss the expected energy dependence of the observable quantities, and present predictions for the experiments at 2.76, 13 and 14 TeV.

Keywords: <pp scattering ; hadronic collisions>
PACS: 13.85.-t,13.85.Lg,13.85.Tp,13.85.Dz

GENERAL INFORMATION AND DATA ANALYSIS

We establish explicitly disentangled real and imaginary amplitudes for pp elastic scattering based on a QCD motivated model. With impact parameter representation $(s,\vec{b})$ and its Fourier transform in $(s,\vec{q})$ space both represented by simple analytical forms, we are able to control unitarity and dispersion relation constraints, and provide geometric interpretation of the interaction range. The regularity obtained in the description of the data and the physical interpretation give reliability to the proposed amplitudes.

The amplitudes of pp elastic scattering originally constructed through profile functions in b -space are written

$$\widetilde{T}_K(s,\vec{b}) = \frac{\alpha_K}{2\beta_K} e^{-b^2/4\beta_K} + \lambda_K(s)\widetilde{\psi}_K(\gamma_K(s),b) \ , \tag{1}$$

with the usual Gaussian forms plus the characteristic shape functions

$$\widetilde{\psi}_K(s,b) = \frac{2e^{\gamma_K - \sqrt{\gamma_K^2 + b^2/a_0}}}{a_0\sqrt{\gamma_K^2 + b^2/a_0}} \left[1 - e^{\gamma_K - \sqrt{\gamma_K^2 + b^2/a_0}}\right] . \tag{2}$$

The label $K = R, I$ indicates either the real or the imaginary part of the complex amplitude.

For large b, corresponding to peripheral collisions, the amplitudes fall down with a Yukawa-like tail, $\sim (1/b)\exp(-b/b_0)$, that reflects effects of virtual partons (modified gluon field) at large distances in the Stochastic Vacuum Model [1].

The comparison with $d\sigma/dt$ data and determination of parameters are made with the amplitudes in t-space. The quantities $\Psi_K(\gamma_K(s), t = -\vec{q}_T^{\,2})$ obtained by Fourier transform of Eq. (1) are written

$$T_K^N(s,t) = \alpha_K(s)\mathrm{e}^{-\beta_K(s)|t|} + \lambda_K(s)\Psi_K(\gamma_K(s),t) \ , \tag{3}$$

and the shape functions converted to $t-$ space take the form

$$\Psi_K(\gamma_K(s),t) = 2\ \mathrm{e}^{\gamma_K} \left[\frac{\mathrm{e}^{-\gamma_K\sqrt{1+a_0|t|}}}{\sqrt{1+a_0|t|}} - \mathrm{e}^{\gamma_K}\ \frac{e^{-\gamma_K\sqrt{4+a_0|t|}}}{\sqrt{4+a_0|t|}}\right] . \tag{4}$$

The complete analysis of elastic scattering [2, 3, 4] requires also the contributions from the Coulomb interaction at small $|t|$ and from perturbative 3-gluon exchange at large $|t|$. The fixed parameter $a_0 = 1.39\ \mathrm{GeV}^{-2}$ is given by the correlation length of the gluon condensate. All parameters have been determined as smooth functions of s and the properties of the amplitudes (magnitudes, signs, zeros) have been described in detail [5].

In our normalization the elastic differential and the total cross sections are written

$$\frac{d\sigma(s,t)}{dt} = (\hbar c)^2[T_I^2(s,t) + T_R^2(s,t)] = \frac{d\sigma^I(s,t)}{dt} + \frac{d\sigma^R(s,t)}{dt} \quad , \quad \sigma(s) = (\hbar c)^2\ 4\sqrt{\pi}\ T_I^N(s,t=0) \ . \tag{5}$$

Differential Cross Sections and Amplitudes in the 1.8 to 14 TeV Range

In Fig. 1 we show the predictions of $d\sigma/dt$ for the LHC energies 2.76 , 8 , 13 and 14 TeV. In the RHS we use the energy $\sqrt{s} = 8$ TeV as an example to show the imaginary and real nuclear amplitudes $T_I^N(s,t)$, $T_R^N(s,t)$ as functions of $|t|$ as predicted by Eq.(3,4). The interplay of the imaginary and real amplitudes at mid values of $|t|$ is responsible for the dip-bump structure of the differential cross section, that was shown before [3] for $\sqrt{s} = 7$ TeV. For $|t| \geq 1.5\,\mathrm{GeV}^2$ the real part becomes dominant, with positive sign.

Our description [3] of the elastic scattering data at 7 TeV from the TOTEM Collaboration [6] reproduces N=165 points in $d\sigma/dt$ with an impressive squared average relative deviation $< \chi^2 >= 0.31$. Characteristic quantities at this energy are $\sigma = 98.65$ mb, $\sigma_{\mathrm{el}} = 25.39$ mb , $B = 19.90$ GeV^{-2}, that compare extremely well with the values $\sigma = 98.6 \pm 2.2$ mb, $\sigma_{\mathrm{el}} = 25.4 \pm 1.1$ mb , $B = 19.9 \pm 0.3$ GeV^{-2} published by TOTEM.

Preliminary data for $d\sigma/dt$ at 8 TeV

The preliminary TOTEM data of $d\sigma/dt$ at 8 TeV seem to be regular enough for our analysis. The data discussed below are taken (reading by eye) from slides of talks by members of the TOTEM Collaboration [7].

As far as we can read from the presentation slides, we identify 212 data points in three sets : 1) N=97 points in the forward interval $6 \times 10^{-4} \leq |t| \leq 0.02$ GeV^2 ; 2) N=45 points in an intermediate interval $0.08 \leq |t| \leq 0.3$ GeV^2 ; 3) N=70 points in a mid $|t|$ range $0.3 \leq |t| \leq 0.95$ GeV^2. This information is transferred to the plot in Fig. 2, together with our calculation. The quality of the representation seems to be equivalent to that of our treatment of the 7 TeV data.

Our values for B_I and B_R lead to the $d\sigma/dt$ effective slope $B = [B_I + \rho^2 B_R]/[1+\rho^2]$ equal to $B = 20.405$ GeV^{-2}.

Hopefully the analysis of the final TOTEM measurements will be more precise and will confirm the validity of our description for 8 TeV and predictions for 13 and 14 TeV .

Inelastic and Total Cross Sections

For the inelastic cross section we assume the difference $\sigma_{\mathrm{inel}} = \sigma - \sigma_{\mathrm{el}}$ and then we have 73.26 mb at 7 TeV.. Published values of the TOTEM Coll. using different methods are 73.15 ± 1.26 [6], 73.7 ± 3.4 [8] and 72.9 ± 1.5 [9]. ALICE Coll. [10] gives $\sigma_{\mathrm{inel}} = 73.2 \pm 5.3$ mb , and ATLAS Coll. $\sigma_{\mathrm{inel}} = 69.4 \pm 2.4 \pm 6.9$ mb [11]. There are also CMS results [12] with non-informed missing contributions. In these measurements there are extrapolations using Monte Carlo models to include diffractive events of low mass. All these results are compatible with our calculations.

A measurement to be compared with our predictions is the $\sqrt{s} = 2.76$ TeV value of ALICE Coll., that gives $\sigma_{\mathrm{inel}} = 62.8 \pm 4.2$ mb , while we have the compatible value 63.11 mb.

The analysis of compatibility for the 1.8 TeV measurements of σ_{inel} by CDF and E811 in Fermilab [13] suggests the value $(1+\rho^2)\sigma_{\mathrm{inel}} = (60.3 \pm 2.3$ mb, that with our ρ value gives $\sigma_{\mathrm{inel}} = (59.1 \pm 2.3$ mb. We have 58.89 mb for 1.8 TeV, once more in very good agreement.

At 57 TeV the Auger Cosmic Ray experiment [14], using other models for pp input, obtains $\sigma_{\mathrm{inel}} = 92 \pm 14.8$ mb , while our extrapolation gives 101 mb. This measurement [15] is discussed together with other CR Extended Air Showers (EAS) experiments, using our inputs and a basic Glauber method to connect pp and p-air processes. Our calculation reproduces well all CR data for p-air cross sections with energies $\sqrt{s}$ (in the pp system) up to 100 TeV.

For 8 TeV we have predictions $\sigma = 101.00$ mb , $\sigma_{\mathrm{el}} = 26.18$ mb , $\sigma_{\mathrm{inel}} = 74.82$ mb , $\sigma_{\mathrm{el}}/\sigma = 0.26$. The measurements by TOTEM [16] give for the same quantities $\sigma = 101.7 \pm 2.9$ mb , $\sigma_{\mathrm{el}} = 27.1 \pm 1.4$ mb, $\sigma_{\mathrm{inel}} = 74.7 \pm 1.7$ mb, $\sigma_{\mathrm{el}}/\sigma = 0.266 \pm 0.006$.

All this information show that our formulae $d\sigma/dt$ at 8 TeV and for the energy dependence of σ and σ_{inel} in pp scattering work very well.

Remarks and Comments

The proposed amplitudes have simple forms, evaluated with few operations with elementary functions. The shape of the dip-bump behavior results from a delicate interplay of the imaginary and real amplitudes. All intervening quantities

and derived properties present smooth energy dependences. The zeros of the real and imaginary parts have very regular displacements, converging to finite limits as the energy increases, showing remarkable connection with positions and heights of dips, bumps and inflections in $d\sigma/dt$.

The slopes B_I and B_R at the origin, with their characteristic difference in values, together with the ratio ρ, are essential quantities in the definition, through the unique analytical forms of the amplitudes, of the properties of the observed $d\sigma/dt$ in the whole t range. Their values are thus fixed with high accuracy. It is important that the slopes show quadratic dependence in $\log s$, instead of the linear dependence suggested by Regge phenomenology.

The integrated elastic cross sections are evaluated in their separate parts, obtained from the real and imaginary amplitudes, and are also represented by simple parabolic forms in $\log s$.

The properties of ratios (with respect to the total cross section) of slopes and of integrated elastic cross sections, that tend to finite asymptotic limits, show that the hypothesis of a black disk limit in the behaviour of the pp interaction seems to be excluded by phenomenology.

Taking into account previous publications at 1.8 and 7 TeV, we obtain cross sections and amplitudes at 2.76, 8 , 13 and 14 TeV, with no free numbers. Future data will test.

We also discuss the geometrical interpretation of our amplitudes, showing that the effective interaction radius in b-space increases with the energy. Our amplitudes obey a geometric scaling in asymptotic energies, and indicate that the profile function $d^2\sigma_{\rm inel}/d^2\vec{b}$ tends to a universal (energy independent) function with respect to a scaling variable, $x \sim b/\sqrt{\sigma}$. This universal function exhibits a considerable diffused surface, indicating a scenario different from the commonly accepted black disk. At LHC energies, the saturation seems to start (the central value of $d^2\sigma_{\rm inel}/d^2\vec{b}$ is almost unity), but the asymptotic profile is still far and only can be reached for $\sqrt{s} > 10^4$ TeV. The connection between the diffused surface of long range and inelastic diffractive processes will be an interesting line of investigation.

We believe that our analytic representation of the scattering amplitudes will serve as important guidance for the future measurements in LHC, and also for a theoretical understanding of the intermediate region of partonic saturation phenomena.

At this Diffraction 2014 conference related work on the black-disk behaviour [17] and on the determination of pp amplitudes at LHC energies [18, 19] were presented, showing that this is an important field of research at the present.

ACKNOWLEDGMENTS

The authors wish to thank the Brazilian agencies CNPq, PRONEX , CAPES and FAPERJ for financial support.

REFERENCES

1. H.G. Dosch, *Phys. Lett. B* **190**, 177 (1987); H.G. Dosch, E. Ferreira, A. Kramer *Phys. Rev. D* **50**, 1992 (1994).
2. E. Ferreira and F. Pereira, *Phys. Rev. D* **59** , 014008 (1998) ; *Phys. Rev. D* **61**, 077507 (2000).
3. A. Kendi Kohara, E. Ferreira and T. Kodama , *Eur. Phys. J. C* ,**73**, 2326 (2013).
4. A. Kendi Kohara, E. Ferreira and T. Kodama , Phys. Rev. D **87**, 054024, (2013).
5. A. Kendi Kohara, E. Ferreira and T. Kodama , *Eur. Phys. J. C* (2014), arXiv: 1408.1599 [hep-ph] .
6. G. Antchev et al., Totem Coll., Eur. Phys. Lett. **101**, 21002 (2013)
7. M. Deile, Totem Coll., Talk at DIS 2014 (Warsaw, April 2014); J. Kaspar, Totem Coll., talk at XXX-th International Workshop on High Energy Physics, Protvino, June 2014.
8. G. Antchev et al., Totem Coll., Eur. Phys. Lett. **101** (2013) 21003.
9. G. Antchev et al., Totem Coll., Eur. Phys. Lett. **101** (2013) 21004.
10. B. Abelev et al., ALICE Coll., Eur. Phys. J. C (2013) 73:2456.
11. G. Aad et al., Nature Commun. 2:463 (2011).
12. S. Chatrchyan et al., CMS Coll., Phys Lett B **722** (2013) 5.
13. S. Klimenko, J. Konigsberg and T. M. Liss, FERMILAB-FN-0741 (2013).
14. P. Abreu et al , Auger Coll., Phys. Rev. Lett. **109**, 062002 (2012).
15. A. Kendi Kohara, E. Ferreira and T. Kodama , arXiv: 1406.5773 [hep-ph] ; J. Phys. G **41** , 115003 (2014).
16. G. Antchev et al., Totem Coll., Phys. Rev. Lett. **111** (2013) 012001
17. D.A. Fagundes, M.J. Menon, P.V.R.G. Silva, J. Phys. G40 (2013) 065005 ; ibid : arXiv : 1410-4423[hep-ph] .
18. C. Bourrely, J.M. Myers, J.Soffer and T.T. Wu , *Phys. Rev.D* **85**, 096009 (2012).
19. O.V. Selyugin, *Eur. Phys. J. C*(2012), 72:2073 ; talk presented at Diffraction 2014 .

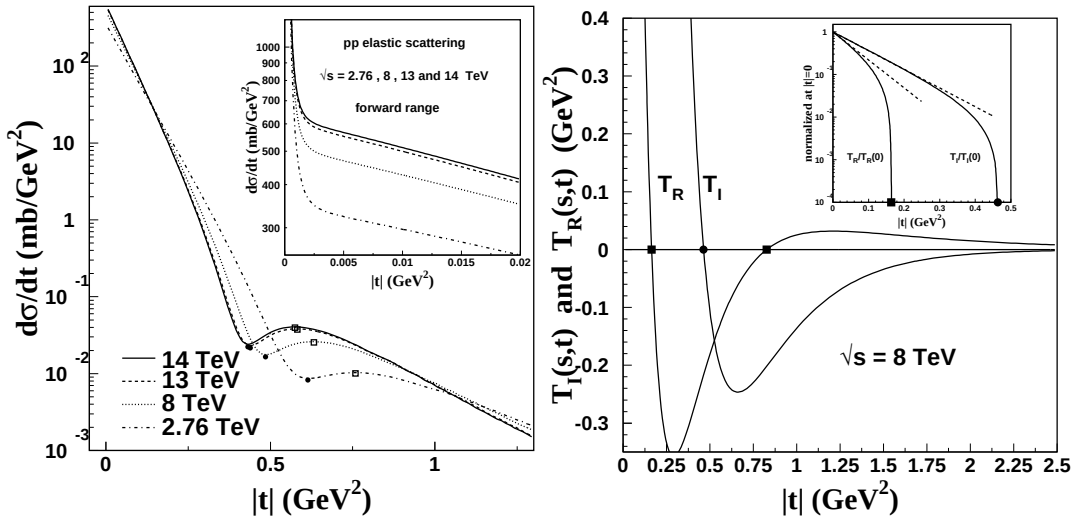

FIGURE 1. (LHS) - Values of $d\sigma/dt$ obtained for energies of LHC experiments. The positions of dips and bump peaks, marked with dots and squares, displace to the left as the energy increases, and can be connected with straight lines. The inset shows the low $|t|$ range, with Coulomb interaction effects included. (RHS) - Real and imaginary parts of elastic pp scattering amplitude at 8 TeV, as functions of $|t|$. The general behaviour is the same for all energies, with one and two zeros respectively for the imaginary and real parts. The behaviour for small $|t|$ is shown in the inset, indicating the difference of slopes B_R and B_I, and the deviations of the exponential forms that occur as $|t|$ increases, each amplitude going towards its zero. A second zero of the imaginary part occurs at much higher $|t|$.

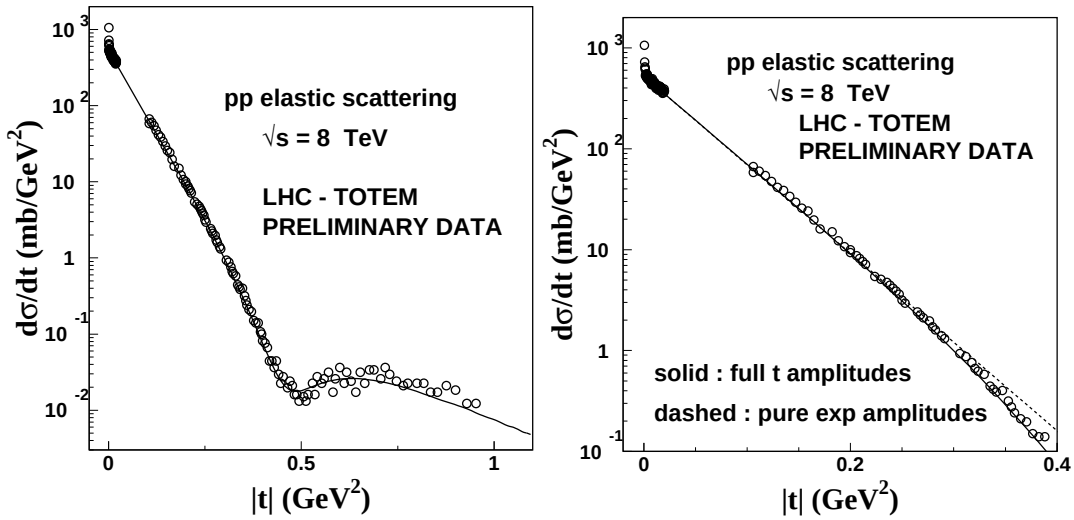

FIGURE 2. Preliminary data at 8 TeV extracted by eye from presentation slides of the TOTEM collaboration plotted together with our predicted representation for $d\sigma/dt$. In the RHS we plot the forward range, with the dashed line for pure exponential amplitudes.